Physics and Philosophy — Issn: 1863-7388 — 2006 — Id: 002

Article

Detection of High-Energy Particles: The Eyes of the Experimental Particle Physicist

Thomas Lohse
(Humboldt-Universität, Department of Physics, Newtonstr. 15, D–12489 Berlin, Germany)

Abstract: In spite of quantum field theoretical and philosophical problems to define the concept of elementary particles and to understand their localizability, particles become intuitively apparent by the traces they leave in particle detectors. Today, experimental particle physicists have reached a high degree of perfection in measuring and visualizing particles up to highest energies using a variety of high technology detection devices and sophisticated, powerful particle accelerators. The paper reviews the basic detection techniques and puts the microscopic quantum field theoretical processes of interest into perspective with the measurements performed at macroscopic scales. It is shown that particle detectors and accelerators are highly classical devices which localize particles without significantly affecting the tails of their wave functions. It is discussed which properties of particles can be measured and how these measurements relate to the dynamics of elementary particles at microscopic length scales.

Keywords: relativistic particles, particle localizability, particle detectors

1 Introduction

The goal of experimental particle physics is to probe the structure of matter and the forces between elementary particles with steadily increasing resolution. For this purpose, the interactions of high-energy particles, created in terrestrial particle accelerators or provided by extraterrestrial cosmic rays, are measured with sophisticated detection devices, able to record final state particles produced in the interactions. The spatial extent of the interaction region scales like the inverse of the momentum transfer. Todays experiments are sensitive to processes at a scale of 10^{-18} m, roughly one thousands of the proton radius. At such scales, quantum fluctuations are important and experiments therefore allow subtle (loop level) tests of quantum field theories. On the other hand, the particle notion

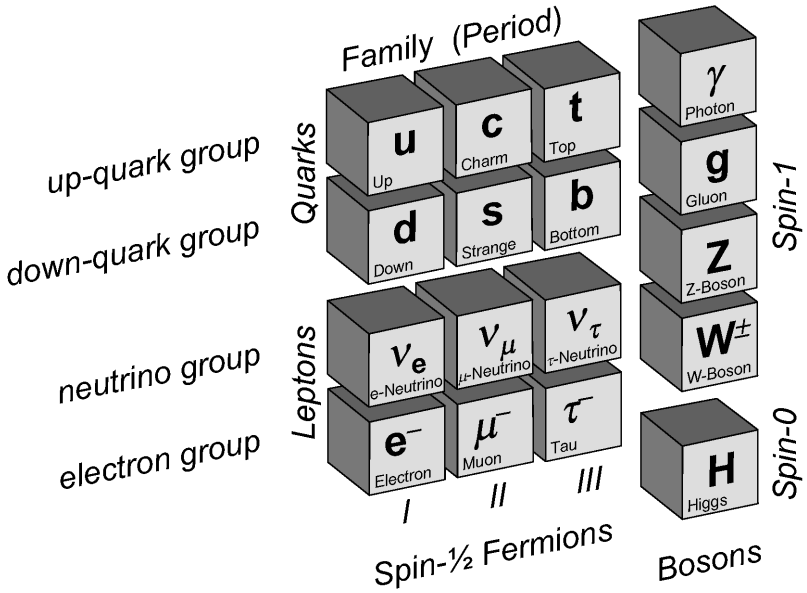

Figure 1: Fundamental particles and fields in the standard model of particle physics.

is fuzzy in quantum field theory (Fredenhagen/Rehren/Seiler, 2006). Moreover, the localizability of high-energy, relativistic particles is problematic and heavily debated (Hegerfeld, 2001). Experimentally, however, objects which can be intuitively identified as high-energy particles are made clearly visible and can be well localized in space, momentum, time, energy, mass and charge using particle detectors.

This article is intended to help resolving this apparent contradiction by clarifying the process of particle detection and the measurement of particle properties. It will be shown that only a small class of particles can actually be measured in detectors but that these measurements can be related to the properties of the fundamental matter and force fields at microscopic scales. Some of the most important particle detection techniques will be described, and measurement errors and quantum mechanical uncertainties will be compared. The discussion is illustrated by examples for detectors at highest particle energies presently accessible.

2 Fundamental particles

The experimental particle physicist wants to detect the fundamental particles and fields and measure their properties and interactions. In todays standard model of elementary particle physics there is a surprisingly small number of fundamental particles and fields, as listed in Figure 1. Matter consists of spin-1/2 fermions, the quarks and leptons. They can be arranged into three families, each with two quarks (up-type with electric charge $2/3\,e$ and down-type with electric charge $-1/3\,e$) and two leptons (charged electron-type and neutral neutrino-type), with

periodically repeating dynamical properties. All fermions are accompanied by their anti-particles with the signs of all additive quantum numbers inverted. Quarks appear with three different charges of the strong force (colors) while leptons are not interacting strongly. Matter, as we know it, consists of atoms which contain a tiny and heavy nucleus surrounded by a much larger shell of light electrons. Atomic nuclei are strongly bound systems of protons and neutrons which themselves consist of quarks of only the first family. Hence atoms are built out of the three electrically charged fermions of the first family. In addition, the Universe is filled by the only weakly interacting neutrinos, created in the early phases after the big bang, in stars and supernova explosions and in radioactive decays. The charged fermions of the second and third family do not appear as static constituents of matter. However, they are present on the level of quantum fluctuations and can be artificially created for short times in high-energy particle collisions.

Forces between the fermions are mediated by the exchange of spin-1 field quanta. The massless photon, γ, mediates the electromagnetic force, the eight massless color-charged gluons, g, mediate the strong force, and the massive vector bosons $W^{\pm}$, Z mediate the weak force. Gravity is left out in this discussion since a consistent quantum field theory for its description is still lacking. At presently reachable energy scales, the effect of gravity in particle interactions is expected to be negligible, and no experimental signs of gravitational effects have been seen up to now.

Finally, in the standard model, the masses of fermions and the weak vector bosons are explained by the existence of a background field, the spin-0 field quantum of which is called the Higgs boson, H. This is the only fundamental particle which is still hypothetical and has not yet been found experimentally, although it is known that its mass would have to be larger than $114.4\,\mathrm{GeV}/c^2$ at 95% confidence level (Eidelman et al., 2004).

There are many reasons to believe that the standard model collection of particles is not complete. Theoretically, the introduction of supersymmetry, a symmetry between fermions and bosons, is very attractive. This adds heavy supersymmetric partners to all known particles. Experimentally, it is known that more than 70% of the energy density in the Universe consists of an unknown type of "dark energy". In addition, about 80% of the remaining matter is "dark" and cannot be explained by standard model particles. It is therefore hoped that with the advent of the Large Hadron Collider (LHC) at CERN, new particles will be discovered, possibly supersymmetric, but possibly also of totally unexpected nature. Particle detectors are therefore designed to be broadly sensitive to the detection of new particles and to be able to measure their properties.

3 Detectable particles

It is important to understand what is experimentally meant by the detection of a fundamental particle. It is the exception, not the rule, that fundamental particles can be directly seen. In fact, only the leptons and the photon are directly

detected by their interactions with the detector material. The massive vector bosons $W^{\pm}$ and Z, as well as the Higgs particle, decay almost instantaneously but can be clearly tagged and measured via their decay products. Quarks and gluons (partons) play a special rôle since they carry color charges and can therefore not exist as free particles but only as constituents of color-neutral bound systems, the so-called hadrons. Only at short time and length scales of hard high-energy interactions, partons are quasi-free particles which can be treated by perturbative quantum field theory. Once produced, high-energy partons fragment into collimated bunches of hadrons, the so called jets. Measuring the particles in the jets hence allows to indirectly measure the kinematics of the original partons. In addition the jet structure correlates with the parton type so that at least in some cases the identity of the mother parton can be resolved.

Among the many types of hadrons produced by quarks and gluons, only few live long enough to be directly visible in a detector. All the others are at least in principle detectable by their decay products. A few examples are given in Figure 2.

The most abundant hadrons in jets are the pions, consisting of a quark and an antiquark of the first family, and to a lesser extent the kaon K, which contains one quark (antiquark) from the first family and one strange antiquark (quark) from the second. As an example, the charged pion, $\pi^{\pm}$, has a relatively long lifetime of 26 ns due to the fact that it can only decay via the weak interaction. At typical high energies it therefore travels macroscopic distances before it decays. In a detector a $\pi^{\pm}$ thus appears like a stable particle, leaving ionization tracks and being absorbed in calorimetric devices. The same holds for the charged kaons, $K^{\pm}$. As a second example, the B^0 meson, containing a heavy b-antiquark, also decays weakly. The lifetime is about 1.5 ps, much shorter than that of the pion. Therefore, at typical energies, the B^0 meson decays on average after a flight path of only a few millimeters. In the majority of cases, a D meson, containing a heavy c-antiquark, is created in the decay. It has a similar lifetime as the B^0 meson and again decays after a macroscopic flight path at the millimeter scale. Detection of production and decay vertices separated by millimeters in particle detectors is not an easy task since the closest detector layer is normally still centimeters away from the interaction point, but can be achieved using special high resolution semiconductor vertex detectors, which are by today standard components in particle detectors.

About one third of the pions in a jet are neutral π^0 mesons. Contrary to the charged pions, these can decay electromagnetically (mostly into two photons). The corresponding lifetime is very small, about 0.08 fs. At typical high energies, the π^0 thus decays after a tiny flight path of μm length which cannot be experimentally resolved. A neutral pion is therefore reconstructed by measuring two photons which originate close to the production vertex and have a combined invariant mass corresponding to the mass of the π^0 meson.

Finally, there are a large number of hadron resonances which decay via the strong interaction. An example is the $K^{\star 0}$ meson with a lifetime $\tau = 1.3 \times 10^{-23}$ s. It decays mostly into a π^- meson and a K^+ meson. Typical flight paths have

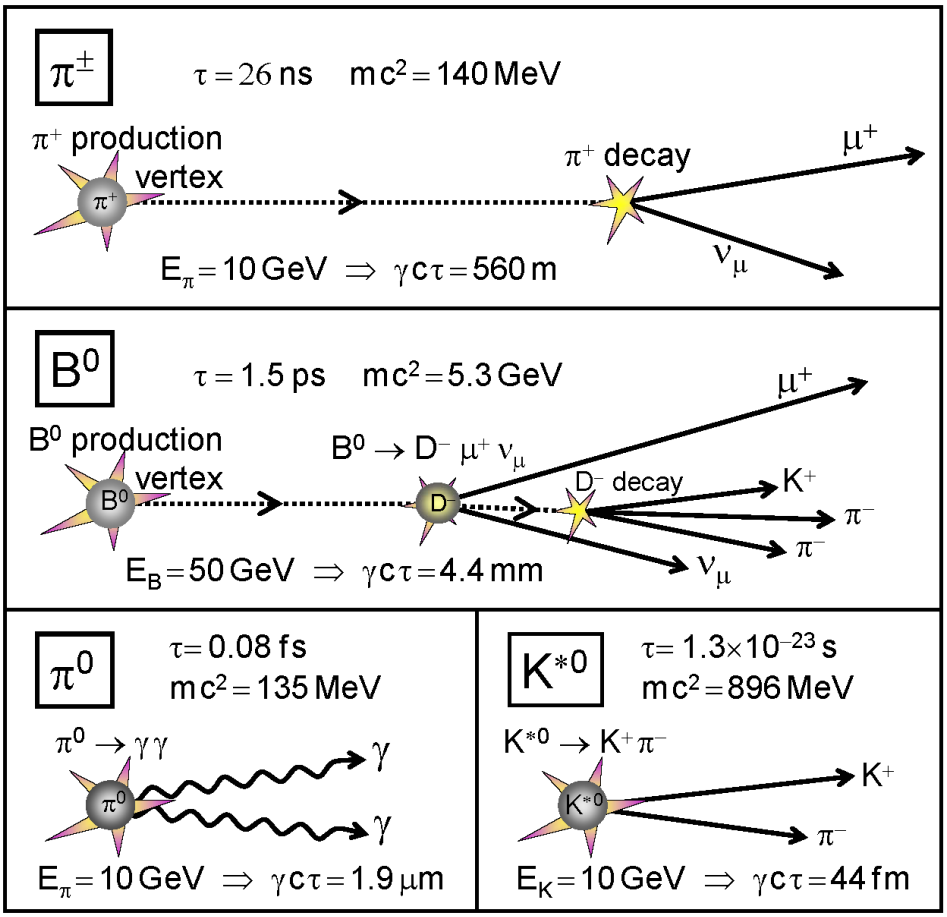

Figure 2: Examples of decays of hadrons produced in high-energy interactions. The production vertex is indicated by a star on the left hand side of each figure, decay vertices by stars further downstream (right hand side). Indicated are rest energies mc^2 and lifetimes τ of the mother hadrons and their mean flight distances in the laboratory till decay, $\gamma c\tau$, assuming typical energies much larger than their rest mass energies and thus a velocity $v \approx c$ (c is the speed of light and γ is the time dilatation factor).

sub-atomic lengths of tens of femtometers, and can hence not be measured by a detector made of matter. The decay products of the $K^{\star 0}$ are, however, both long-lived and are seen in the detector as quasi-stable ionizing particles. The combined invariant mass of the decay products can be measured and corresponds to the mass of the $K^{\star 0}$ meson, however significantly smeared by the Heisenberg energy uncertainty $\hbar/\tau$. Thus, in this case, it is the width of the invariant mass distribution and not the average decay length which gives the experimental handle to measure the lifetime of the particle.

Although the fundamental particles can all be detected directly or by their decay or fragmentation products, it is important to understand the enormous gap in time and length scale between the initial hard interaction process to be studied and the measurement of particles in a detector. This is illustrated by the example of e^+e^- annihilation into a quark and an antiquark, leading to two jets in the final state. Figure 3 displays the different phases of this process.

The electrons and positrons are colliding head-on in the detector system (Figure 3a). This can be achieved by accelerating bunches of typically 10^{11} electrons and 10^{11} positrons to high energies and filling them into so-called storage rings, where they can be kept at constant energy on counter-rotating orbits for hours. The timing is adjusted such that the bunches collide in the center of the detector, occasionally leading to an e^+e^- annihilation event. The typical length of each bunch is 1 cm, such that the interaction time is uncertain by $\delta t \approx \sqrt{2} \times \frac{1\,\mathrm{cm}}{c} \approx 5 \times 10^{-11}\,\mathrm{s}$. The energy spread within a bunch is typically of the order $\delta E \approx 10^{-3} \times E$. Assuming a beam energy of 50 GeV, this leads to $\delta E \times \delta t \approx 2.5 \times 10^{-12}\,\mathrm{GeV\,s} \approx 4 \times 10^{12}\,\hbar$. Similarly, the typical transverse beam dimension multiplied with the spread of transverse momentum of the particles in the beam is huge compared to $\hbar$. In other words, the longitudinal and transverse phase space occupied by the particles in a bunch is macroscopic. The preparation of beams in an accelerator is a process which lies deeply in the classical regime and does not affect the tails of wave functions of the beam particles.

The quark and antiquark are produced in a hard interaction which can be described in perturbation theory by a coherent superposition of amplitudes including all possible quantum fluctuations. Some of the amplitudes are indicated by corresponding Feynman diagrams in Figure 3a. The hard interaction takes place on length scales much smaller than 1 fm, on which the quark and antiquark can be treated as free particles. Once their separation reaches the femtometer scale, a classical strong force field (a so-called color string) builds up between the quark and the antiquark (Figure 3b). When the system expands further, Figure 3c, quark-antiquark vacuum fluctuations are polarized by this color string and the string breaks up into color neutral hadronic clusters from which hadron resonances emerge. On the scale of some 10 fm, Figure 3d, the resonances decay, thus creating the hadrons of the two emerging jets. On average much later, at the μm scale, the neutral pions decay into photons and other electromagnetic decays take place. Hadrons containing heavy quarks decay at typical length scales of millimeters. Zooming further out to the macroscopic scale of a few centimeters (Figure 3e), the final state particles in the jets finally traverse the beam pipe of

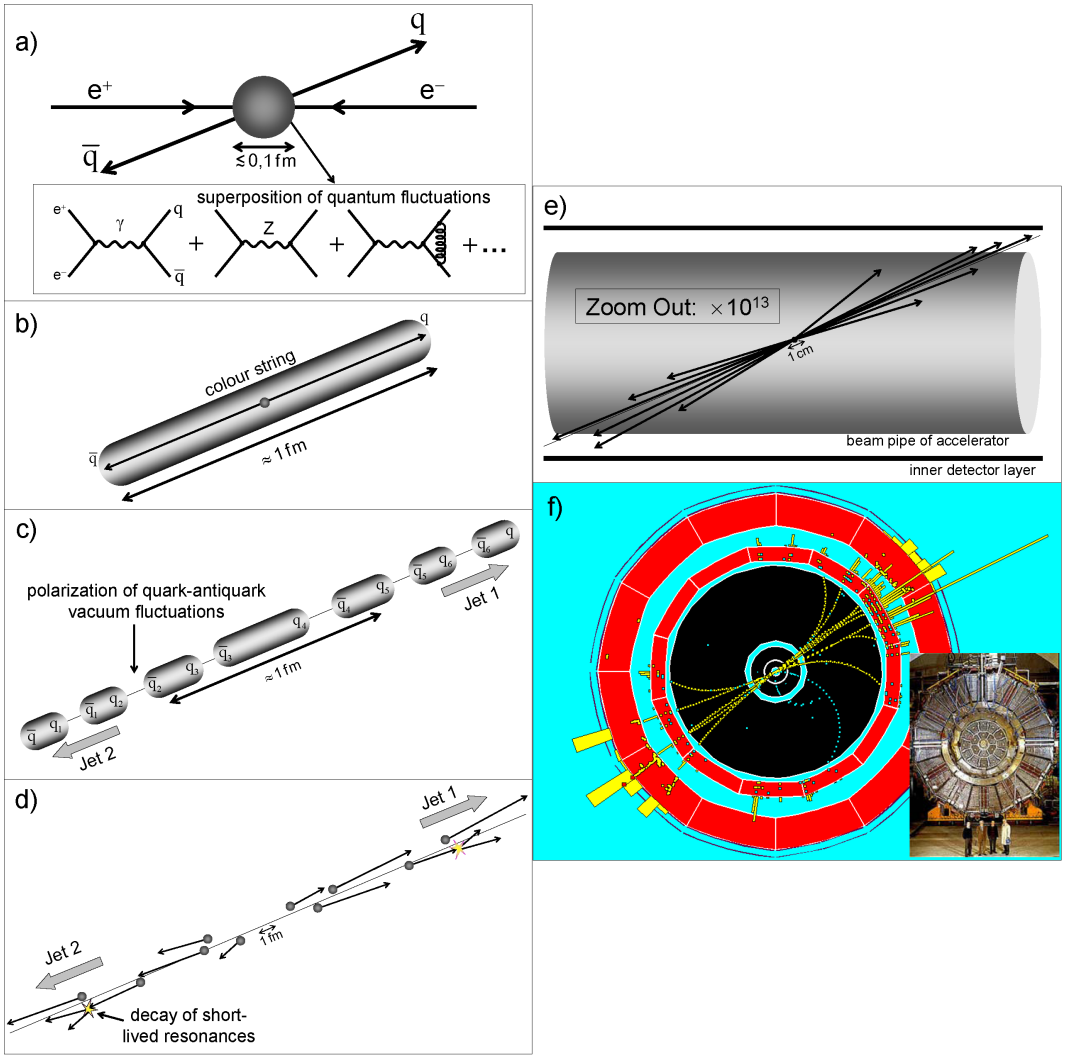

Figure 3: Schematic illustration of the different phases of the development of a two-jet event in e^+e^- annihilation: a) hard interaction, describable as superposition of amplitudes given by Feynman diagrams, b) development of a classical color field (color string) between the two quarks, c) production of color neutral hadronic clusters by polarization of vacuum fluctuations, d) decay of short-lived hadrons, e) development of two back-to-back jets of hadrons, f) measurement in a large particle detector (from CERN, ALEPH experiment, http://aleph.web.cern.ch/aleph/aleph/daligif/dc015768_005906_cal_red_2_w.gif and http://aleph.web.cern.ch/aleph/aleph/alephgif/aleph3.gif).

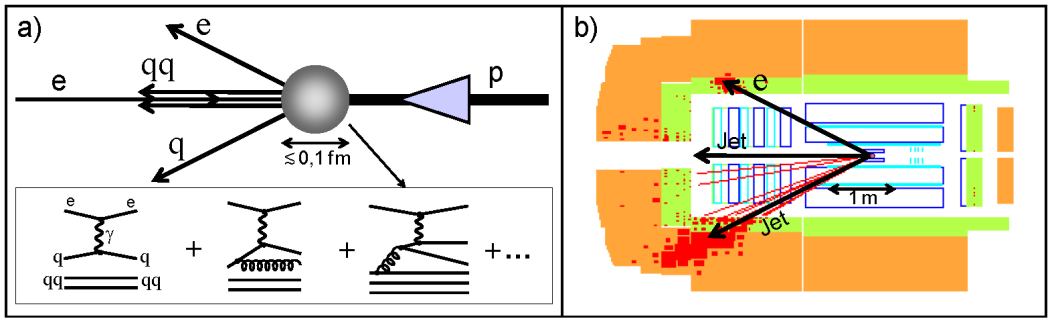

Figure 4: Schematic illustration of a deeply inelastic electron-proton scattering. a. The electron scatters off a quark inside the incoming proton, producing a jet compensating the transverse momentum of the scattered electron. The quarks not participating in the hard interaction continue to move along the flight direction of the incoming proton and produce a second jet, the spectator jet. Some Feynman diagrams for the hard scattering process are indicated. b. Sketch of a real event as seen by the detector H1 at DESY (from http://www-h1.desy.de/pictures/disnc-highq2-86.ps). The directions of the jets and the scattered electron are indicated by arrows.

the accelerator and shortly afterwards the innermost detector layer, typically a semiconductor vertex detector with high spatial resolution. The complete detector has a typical diameter of 20 m. An example of a two jet event as measured in the ALEPH detector at the LEP storage ring at CERN is shown in Figure 3f.

It is not only possible to measure quarks which have been created in a hard interaction but one can also measure quarks inside hadrons. An example is the hard scattering of electrons and protons, as illustrated in Figure 4. Such processes are for example studied at the HERA storage rings at DESY, where 27 GeV electrons (or positrons) collide with 920 GeV protons. In a hard (deeply inelastic) interaction, the electron interacts with a quasi-free quark, mostly by exchange of a virtual photon. The scattered quark recoils against the scattered electron such that the momentum stays balanced. The remaining quarks of the proton are unaffected by the interaction. The scattered quark and the proton remnant finally fragment into two jets which can be recorded in the detector. A typical event, as measured by the H1 detector at HERA, is shown in Figure 4b.

Measuring the momentum of the electron and/or the momentum of the particles in the jet from the scattered quark, one can determine the kinematics of the quark both before and after the hard scattering. Measuring a large number of such deeply inelastic events one can hence infer the density of quarks in the proton which carry any fixed fraction of the momentum of the incoming proton, the so-called structure functions.

As in e^+e^- annihilation, such deeply inelastic processes take place on sub-fm length scales, and can be described perturbatively by a coherent sum of amplitudes, some of which are shown in Figure 4a. The virtual photon can either couple to a constituent quark (valence quark) of the proton directly or to a quark involved

in quantum fluctuations, like a valence quark which has emitted a gluon but also a so called sea-quark, created in quark-antiquark fluctuations. This implies that not only the valence quarks but all quarks and antiquarks can be detected inside the proton. However, quantum fluctuations can only be resolved at the length scale given by the wavelength of the exchanged photon which decreases when the momentum transfer in the interaction increases. As a consequence, quantum field theory predicts that the measured quark densities at fixed fractional quark momentum depend on the resolution, i.e. the momentum transfer in the scattering process. This has been quantitatively confirmed by experiments, demonstrating the predictive power of quantum field theory on one side, and the failure of the naive constituent particle picture of the proton on the other.
It should be remarked that such scale dependencies of measurements are quite common in everyday life. The resulting length of the coastal line of the British Island, e.g., depends strongly on the length scale used for the measurement, i.e. the scale below which structures are ignored and smoothed out.

4 Detection techniques

In this section some of the most important detection techniques will be discussed. No attempt is made to give an exhaustive list of detection devices. The discussion rather focuses on representative examples, relevant for understanding the methods for localizing high-energy relativistic particles in space, time, momentum, energy, mass, and charge.

4.1 Interaction of particles with matter in detectors

Final state particles are measured via their interactions with atoms (shell electrons or atomic nuclei) of the detector material. All fundamental forces (weak, electromagnetic, and strong) may be important in these interactions:

- **Electromagnetic interaction:** All charged particles lead to ionization and/or excitation of atoms and molecules or electron-hole creation in semiconductors. In addition charged particles lead to polarization of molecules in the surrounding material which may result in the emission of electromagnetic radiation (Cherenkov radiation, transition radiation). Electrons (and to a much lesser extent also heavier charged particles) can radiate hard photons (bremsstrahlung) when deflected by the Coulomb field of a nucleus. Photons are neutral but are also detected through their electromagnetic interaction. When passing through the Coulomb field of a nucleus, they can convert into electron-positron pairs. If the material is dense enough, the electrons and positrons will in term undergo bremsstrahlung, creating new photons. The result is a cascade (shower) of electrons, positrons and photons, a so-called electromagnetic shower. Such showers are initiated by photons, electrons or positrons.

- **Strong interaction:** Hadrons, consisting of quarks, can undergo strong interaction with the atomic nuclei of the detector material, producing more hadrons. If the material is dense enough, these hadrons can undergo nuclear interactions again, such that a hadronic cascade (shower) builds up. Hadron cascades are very different from electromagnetic cascades. Electromagnetic cascades are spatially compact and regular, while hadronic cascades are long, broad and very irregular, exhibiting large fluctuations of energy deposit.

- **Weak interaction:** Neutrinos only interact weakly. Therefore the vast majority of neutrinos escapes a detector without a trace. In special applications, the detector is exposed to a strong neutrino flux for sufficiently long times, so that nevertheless a sizable number of neutrinos is detected when they undergo weak interaction either with the atomic nuclei of the detector material or electrons in the atomic shells. In such interactions, neutrinos may convert into charged leptons which are seen in the detector due to ionization or shower production. In addition, detectable secondary particles are created when the nucleus or shell electron is hit.

4.2 Spatial localization of particles

A classic example for a detector for charged particles is the photographic emulsion which is "exposed" by the passage of an ionizing particle like a photographic film is exposed by visible light. After development of thin slices of the emulsion, the particle trajectories become visible as chains of small silver grains (Figure 5), leading to a spatial resolution of the order of 1 μm, better than reachable by any modern high technology device.
Unfortunately the emulsion detector is not useful for typical high speed and high rate applications of most modern experiments, since the emulsion can only be exposed once for a certain period of time and then has to be developed and scanned. Most particle detectors today require, however, online detection and fast automatic recognition of interesting (often rare) event classes. Therefore todays particle detectors mostly rely on components which produce electric signals which can be directly processed by fast electronics, digitized and sent to computers.
A prominent example of a tracking detector with electronic read-out is the multi-wire proportional chamber (Figure 6). It consists of thin anode wires supported inside a volume filled by an appropriate chamber gas and surrounded by cathode structures, like plates, boxes or cathode wires. The material budget of support structures is kept as low as possible in order to minimize the multiple scattering and ionization losses of a passing charged particle of high energy. Such a particle mainly ionizes the atoms in the gas along the flight path, setting free clusters of electrons. These electrons are accelerated in the electric fields towards the nearest anode wire, where they gain enough energy to produce an ionization avalanche which constitutes enough charge to be electronically detected on the anode wire. The total charge signal is proportional to the primary ionization, which can thus be measured simultaneously. The spatial resolution of such a device depends on

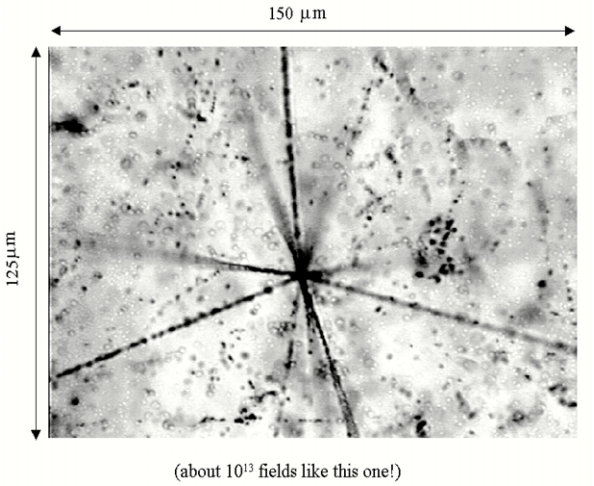

Figure 5: Particle interaction in a thin slice of a chemically developed photo emulsion. The black tracks consist of silver grains lining up along the flight paths of ionizing charged particles created in the interaction. Picture taken from CERN, CHORUS experiment (http://choruswww.cern.ch/Public/techniques/tracks.html).

the anode wire spacing and lies typically in the millimeter range. If one also measures the drift time of ionization charges, i.e. the time between the particle passage and the creation of a charge pulse on the wire, one can improve the spatial resolution to about 100 μm. In this case such a device is called "drift-chamber".

An extreme example of a drift chamber is the time projection chamber (TPC), schematically shown in Figure 7. In this case the chamber consists of a large drift volume inside a field cage filled with a chamber gas. Electrons produced by ionizing particles drift along the homogeneous electric field created by electrodes on the inside of the field cage, allowing for drift lengths up to several meters. Charge detectors – like multi-wire proportional chambers – detect the ionization charges at the end of the drift volume. While the chambers measure transverse coordinates of ionization charges, the measured drift time gives a precise longitudinal coordinate such that a three-dimensional measurement of the ionization track is achieved.

Still higher spatial resolutions can be reached with semiconductor detectors like silicon strip detectors (Figure 8) or silicon pixel detectors. Such detectors consist basically of a high granularity array of individually read out diodes which are completely depleted by a reverse bias voltage. Since the energy needed to produce electron hole pairs in the depletion zone is typically an order of magnitude below that needed for the ionization of chamber gases, the charge yield for a charged particle crossing the detector is large. About 25000 electron-hole pairs are created along a track length of 300 μm, the typical thickness of such devices. This has to be compared to about 100 ions for 1 cm track length if argon under atmospheric pressure is used as chamber gas.

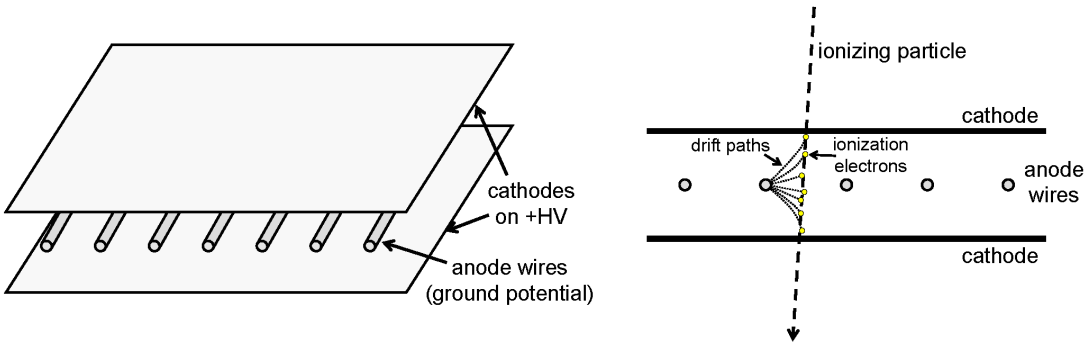

Figure 6: Left: Schematic illustration of a multi-wire proportional chamber, consisting of anode wires between two cathode plates. Right: A charged particle traversing the chamber ionizes the chamber gas. The electrons are accelerated towards the nearest anode wire creating an ionization avalanche close to the wire which in turn leads to a measurable charge signal proportional to the original ionization charge.

The high resolution is achieved thanks to the high granularity of the silicon structure. Strip detectors have typical strip pitches of 20 μm and reach resolutions below 10 μm. However, the number of electronic channels quickly becomes excessive for large detector structures. Therefore, silicon strip and pixel devices are primarily used in the vicinity of the interaction point where the particle density is highest and high spatial resolution is necessary to resolve secondary vertices close to the interaction point.
For illustration, Figure 9 shows the tracks reconstructed with the help of a silicon vertex detector in the ALEPH detector at CERN for an event in which a high-energy electron and a high-energy positron collide and produce two Z-bosons, one decaying into a light quark and its antiquark, the other decaying into a heavy b-quark and a heavy b-antiquark. The jets produced by the heavy (anti)quark each contain a b-hadron with a lifetime of ≈ 1.5 ps, the decays of which lead to slightly displaced secondary vertices, clearly visible in Figure 9.

4.3 Localization of particles in momentum space

The ionization tracks of charged particles in Figure 3f are clearly curved. This is due to the fact that the complete tracking detector is placed inside a large solenoidal magnet providing a homogeneous magnetic field. From the curvature of the tracks, the momentum component perpendicular to the magnetic field, p_T, can be measured. The principle is explained in Figure 10, where the track is measured by two tracking detectors, one in front of and one behind a magnet. From the measurement of the track deflection one can infer the radius of curvature in the magnetic field which in turn is directly connected to the transverse momentum. Since the tracking detectors measure the three-dimensional flight path of charged particles, the complete momentum vector can be derived from the transverse momentum using the measured track inclination. In summary, the

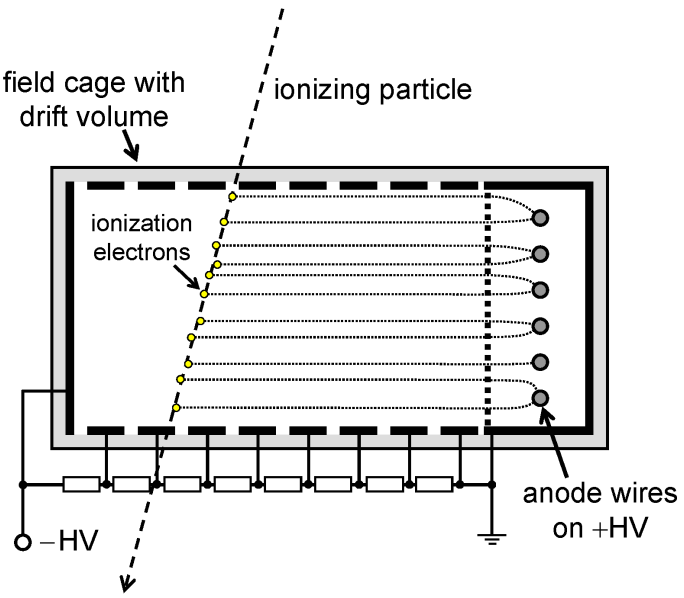

Figure 7: Schematic illustration of a time projection chamber (TPC) as an extreme example of a drift chamber.

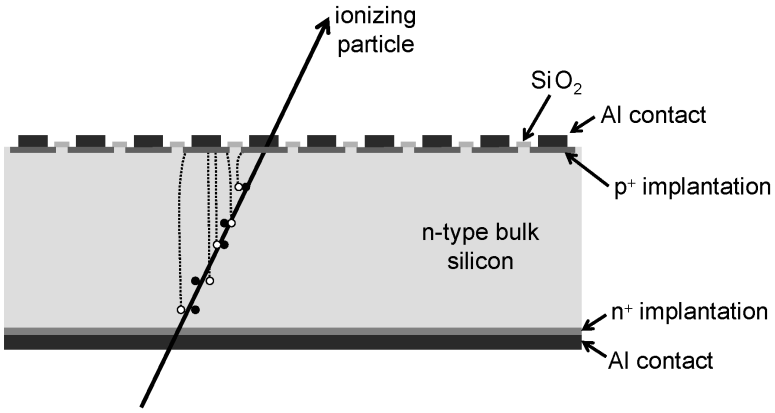

Figure 8: Schematic cross-section of a silicon strip detector consisting of an array of p-n junctions on a bulk of n-doted silicon, completely depleted by a reverse bias voltage. A charged particle traversing the bulk creates 25000 electron-hole pairs on a path length of 300 μm. The holes are drifting to the closest strip and are neutralized, leading to a measurable signal which is spatially well localized.

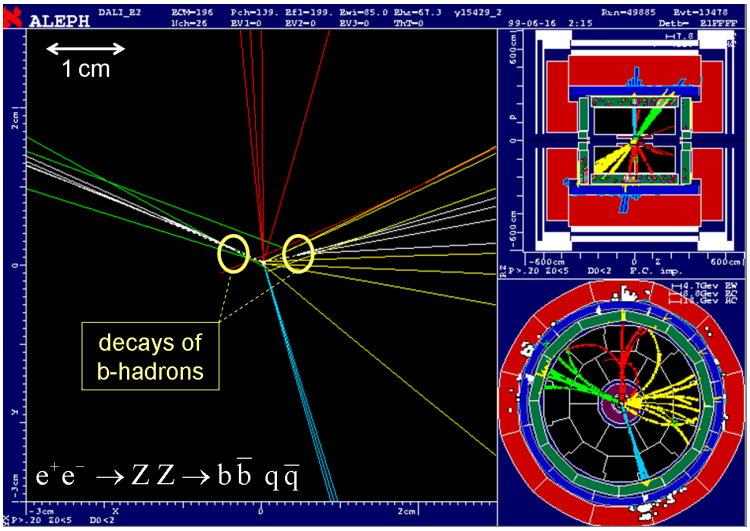

Figure 9: Reconstructed tracks close to the vertex, as measured in an e^+e^- annihilation event with the ALEPH detector at CERN (from http://aleph.web.cern.ch/aleph/dali/192GeV/hqq-49885-013478.ps). Two secondary vertices from decays of b-hadrons are clearly visible.

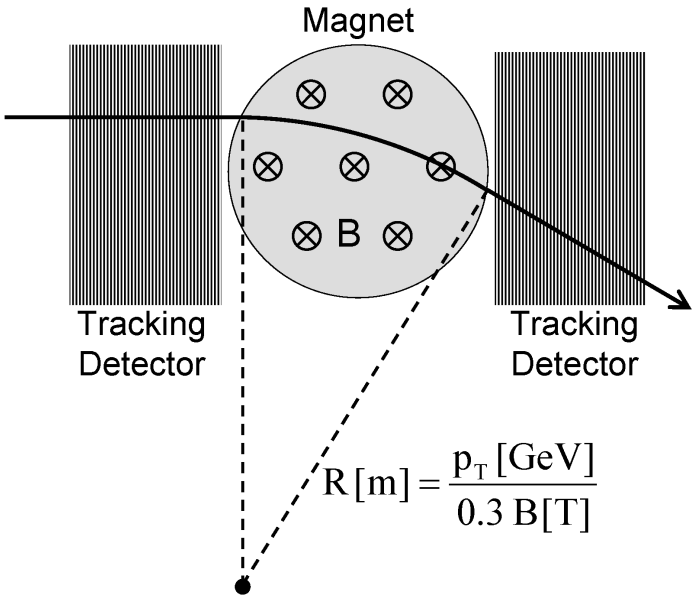

Figure 10: Principle of momentum measurements using two tracking detectors, one in front of and one behind a magnet. The measured radius of curvature, R, of the track is a direct measure for the momentum component, p_T, perpendicular to the magnetic field.

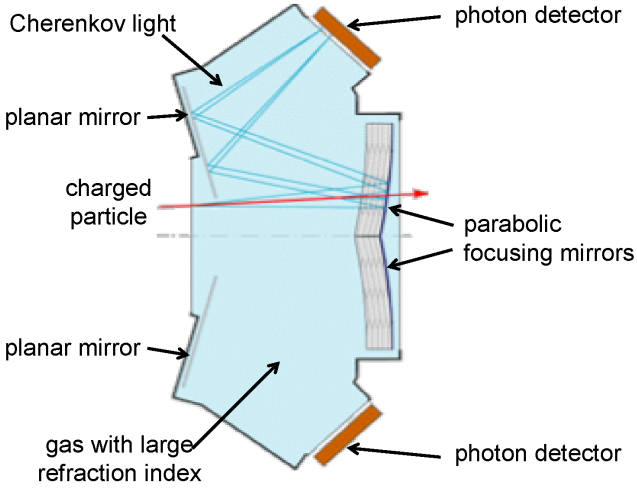

Figure 11: Schematic layout of a ring imaging Cherenkov counter (taken from DESY, Hera-B experiment, http://www-hera-b.desy.de/subgroup/detector/rich/).

shown configuration allows a simultaneous localization of the particle in all three spatial and momentum components.
Note that this fact is far from being in conflict with Heisenberg's uncertainty principle. Uncertainties in spatial coordinates, as given by mechanical precisions of tracking detectors and their resolutions multiply with those of momentum measurements to typically $10^{11}\hbar$ or even larger multiples of $\hbar$. The tracking detectors combined with magnetic fields are therefore operating in the deeply classical regime, hence localizing particles without significantly affecting the tails in their wave functions.

4.4 Particle identification

There is a variety of methods to identify the type of a particle measured in the detector, most of them aiming at measuring the velocity of particles traversing the detector. Combined with the momentum measurement discussed in the last section, the velocity measurement leads to a determination of particle mass and hence to particle identification.
A prominent example for a particle identification detector is the ring imaging Cherenkov detector. It makes use of the bluish Cherenkov light which is emitted in a cone around the flight path of a high-energy particle traversing a medium (often a gas with large refraction index) at a speed larger than the speed of light in the medium. The opening angle of the cone is directly connected to the particle velocity and can for instance be measured by optically focusing the Cherenkov cone into a circle (ring) using parabolic mirrors. The focal plane is equipped with a sensitive photon detector like a matrix of photomultiplier tubes which produce electrical signals proportional to the number of incident photons. A possible layout of the detector is indicated in Figure 11.

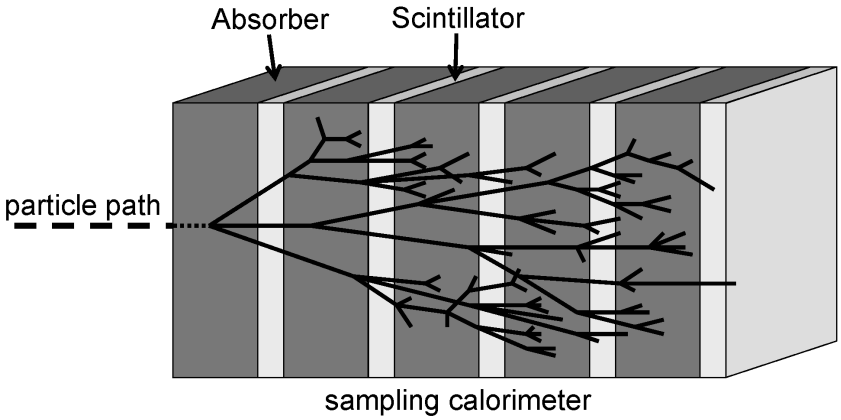

Figure 12: Schematic structure of a sampling calorimeter.

In addition to specialized detectors for particle identification, also ionization densities in tracking chambers can be exploited to determine the velocity and electric charge of a particle, and the measurement of the direction of curvature in a magnetic field reveals the sign of the charge.

4.5 Localization of particles in energy space

The detectors discussed up to now are optimized to measure particle properties via interactions with detector material in which the high-energy particles suffer only small energy losses and angular deflections which can be taken into account in the reconstruction algorithm. The philosophy changes completely for devices which measure particle energies. In this case, massive and dense detector components, so-called calorimeters, are employed which are thick enough to completely absorb the incoming particle by the creation of electromagnetic or hadronic showers.

Figure 12 displays the schematic layout of a sampling calorimeter in which layers of passive absorber material are interspersed with active detector layers. High-energy particles interact mainly in the dense absorber material creating a particle cascade. In the case of electromagnetic detectors, measuring high-energy photons, electrons and positrons, dense materials with a large nuclear charge number Z (like lead) are used in order to create compact electromagnetic showers. In the case of hadronic calorimeters, measuring high-energy hadrons of all types, dense materials with large nuclear mass number A (like iron or uranium) are used for the creation of hadronic showers which are much less compact than electromagnetic showers. Signals are produced in active detector layers between the absorbers, like scintillator layers in which scintillation light is produced upon the passage of charge particles. The light is extracted and collected on photon detectors like photomultipliers. The summed electrical signals in the photon detectors are proportional to the energy of the incident particle absorbed in the calorimeter. The proportionality factor has to be determined in a dedicated calibration procedure.

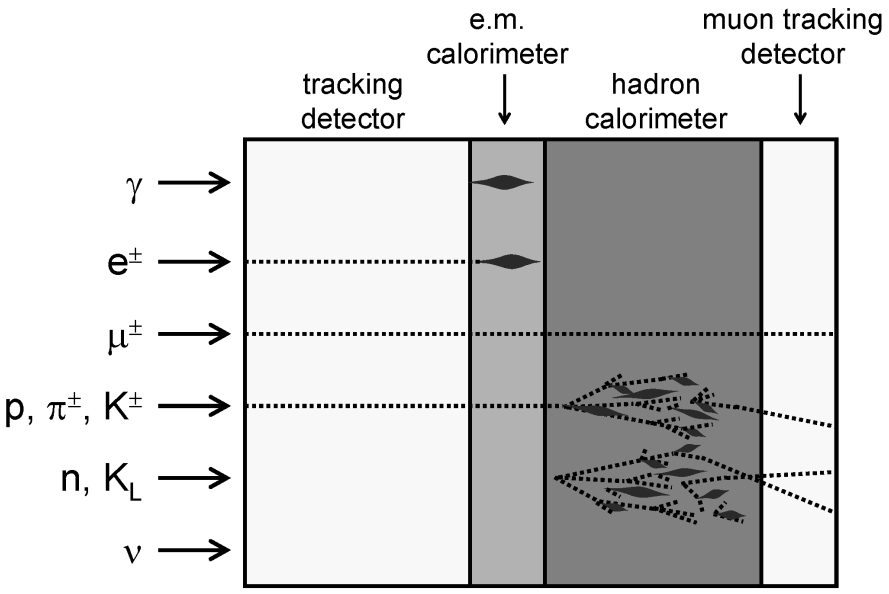

Figure 13: Signatures of final state particles in a typical multi-component detector. Innermost sub-detectors, closest to the interaction point, are on the left, outermost sub-detectors on the right.

Typical energy resolutions are $\delta E/E \approx 10\%/\sqrt{E\,[\mathrm{GeV}]}$ for electromagnetic calorimeters and $\delta E/E \approx 50\%/\sqrt{E\,[\mathrm{GeV}]}$ for hadronic calorimeters. Energy measurements therefore become more precise at higher energies. Calorimeters and other detectors also yield a very precise measurement of the time of incidence of the incoming particle. However, the uncertainties in energy and time measurements multiply to typically $10^{14}\hbar$, showing that also calorimeters operate in the deep classical limit. While localizing particles in energy and time, they do not affect tails in the particle wave functions.

4.6 Characteristic signatures of particles in detectors

Characteristic signatures of different classes of long-lived final state particles are summarized in Figure 13. Detectors are normally partitioned into different sub-detectors, at storage rings often arranged around the beam pipe in cylindrical layers with planar caps at the two ends, such that most of the solid angle around the interaction point is covered. The innermost detectors are tracking detectors with minimal impact on particle energies and flight directions, followed by electromagnetic and hadronic calorimeters further outside. Often the hadronic calorimeter is made of instrumented iron which at the same time serves as magnetic return flux yoke for a solenoidal coil providing a homogeneous magnetic field in the tracking detector. Outside the calorimeters, additional tracking stations, so-called muon chambers, detect penetrating charged particles.
Electrons, positrons and photons are uniquely identified by characteristic compact electromagnetic showers contained in the electromagnetic calorimeter. While

photons don't create signals in the tracking detector, electrons and positrons are seen as ionization tracks, the sign of the curvature of which serves for telling electrons from positrons.
Long lived hadrons create hadronic showers in the calorimeters. These showers are much more extended than electromagnetic showers such that most of the shower energy is recorded in the hadronic part of the calorimeters. Again, charged hadrons (p, $\pi^{\pm}$, $K^{\pm}$) leave ionization tracks in the tracking detector while neutral hadrons (n, K_L) don't. The different types of charged hadrons can be disentangled on the basis of the measured ionization densities in the tracking chamber or by additional detectors for particle identification.
Muons leave a unique signature in the detector. They are about 200 times heavier than electrons and are therefore inefficient in creating bremsstrahlung. Thus they don't initiate electromagnetic showers. Since muons are leptons, they are not subject to strong interactions and therefore don't initiate hadronic showers either. Hence muons are penetrating and only leave an ionization track in the tracking detector and the calorimeters. If energetic enough, they can penetrate the full length of the calorimeters and can be detected by outside muon chambers.
Finally, neutrinos normally escape completely undetected. The presence of neutrinos and their momenta and energies can however still be inferred from the energy-momentum balance measured in the final state.

5 Experiments at the end of the energy scale

During the years, particle accelerators have become more and more powerful both in beam energy and achievable collision rates. The state of the art machine is the Large Hadron Collider (LHC) at CERN which is in the final construction phase and will provide head-on collisions of 7 TeV protons every 25 ns. The LHC is exploring particle physics at the TeV scale and detectors have to be able to cope with extremely high particle densities and have to precisely measure particles up to this energy range. As a consequence, detectors have to have very high granularity and have to be large in order to provide a large lever arm for track measurements and to totally absorb particles in the calorimeters. Figure 14 shows a sketch of ATLAS, one of the large multi-purpose detectors at the LHC. The detector concept is very similar to that shown in Figure 13 but with a length of ≈ 46 m and a height of ≈ 24 m it is much larger than any accelerator-based detector built up to now. ATLAS weighs about 7000 t, a quite moderate weight given its enormous volume. In total about 10^8 electronic channels have to be read out, representing a major challenge for triggering, data acquisition, data storage and data distribution for analysis.
Particle energies much larger than those which can be created on earth by particle accelerators are naturally provided by the cosmic rays bombarding the earth from all directions. They consist mainly of protons and heavier nuclei with a small admixture of anti-particles, but also have a component of gamma rays, electrons, positrons, and presumably neutrinos. Almost a century of research has led to a precise measurement of the cosmic ray flux for an energy range spanning more

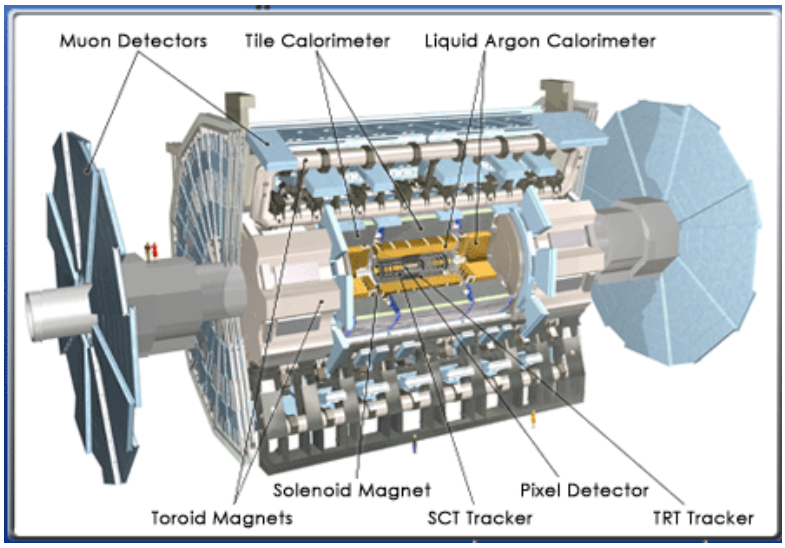

Figure 14: Schematic layout of the ATLAS detector at the LHC at CERN (from http://atlas.ch/atlas_photos.html).

than 10 orders of magnitude, over which the flux varies by more than 30 orders of magnitude, compare Figure 15. The highest energies detected so far are around 10^{20} eV, 7 orders of magnitude higher than the LHC beam energy. Such energies are macroscopic (10^{20} eV = 16 J) but they are nevertheless carried by individual particles, most likely protons, which can be localized in space, time, momentum and energy.

At energies above 10^{12} eV, the cosmic ray fluxes quickly become too small to allow the direct measurement by satellite based detectors. In this case one uses the earth atmosphere as detector medium in which extensive air showers (electromagnetic or hadronic) are created from the interactions of cosmic ray particles with air molecules. The detection systems are placed on the earth surface and employ devices similar to those developed for detectors at particle accelerators. The most important experimental techniques for ground based observation of charged cosmic rays, gamma rays and neutrinos are sketched in Figure 16. Traditionally, extensive air showers induced by cosmic ray hadrons or gamma rays are sampled by surface detector arrays consisting of scintillators or water Cherenkov detectors. Shielded detectors are used to identify muons from the decay of hadrons in hadronic showers. Additional deep underground water or ice Cherenkov detectors can identify muons of higher energies. Specialized detectors, like calorimeters, are used to measure local energy fluxes. Showers can also be measured calorimetrically by collecting the fluorescence light from atmospheric nitrogen, excited by shower particles, in distant wide angle detectors. In addition, air showers can be detected by measuring their radio emission, a technique which will probably play a major rôle in future experiments.

Precise shower reconstruction at low energy thresholds is possible using imaging Cherenkov telescopes, which detect the Cherenkov light emitted in a narrow cone around the shower. High sensitivity, good angular resolution and high separation

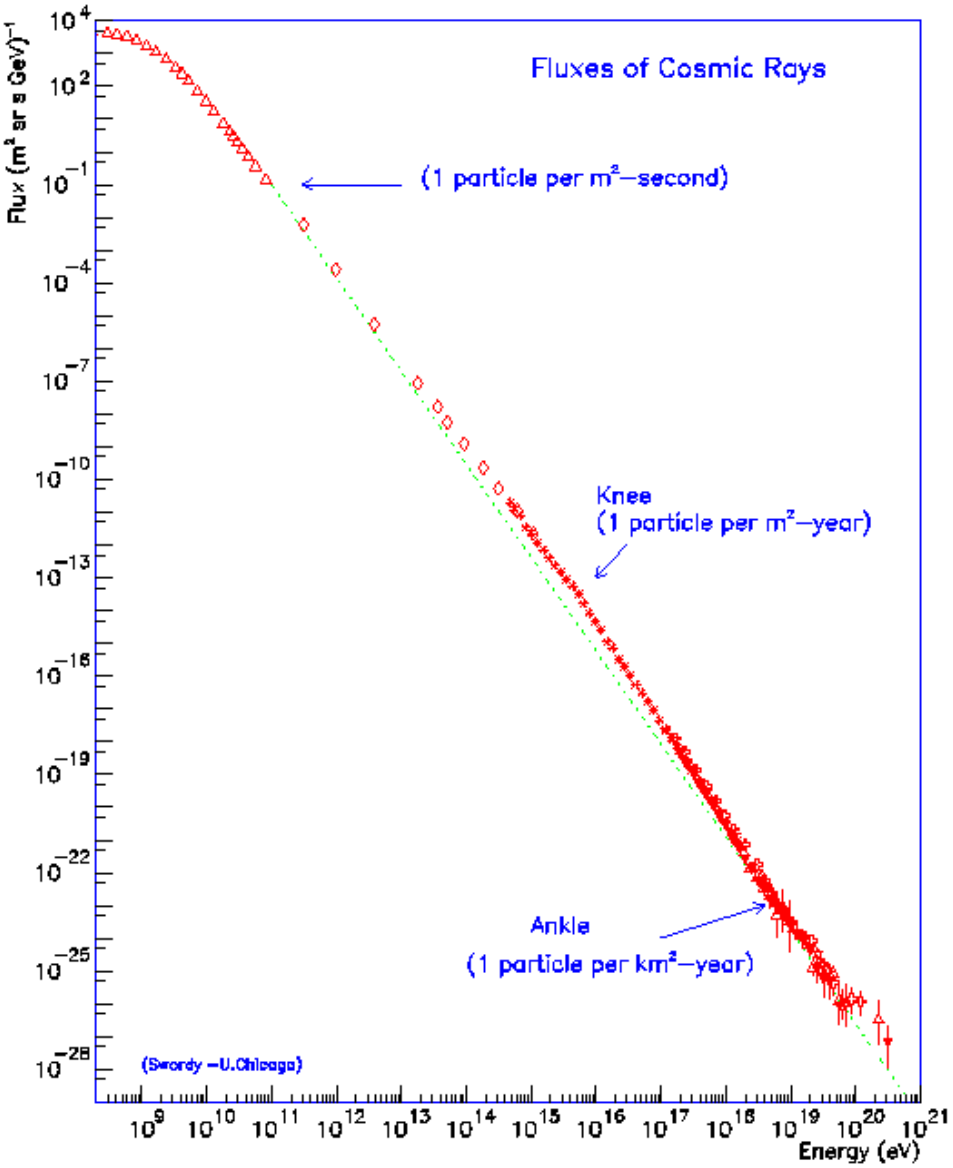

Figure 15: Flux of cosmic ray particles as function of energy (from Cronin/ Gaisser/Swordy 1997).

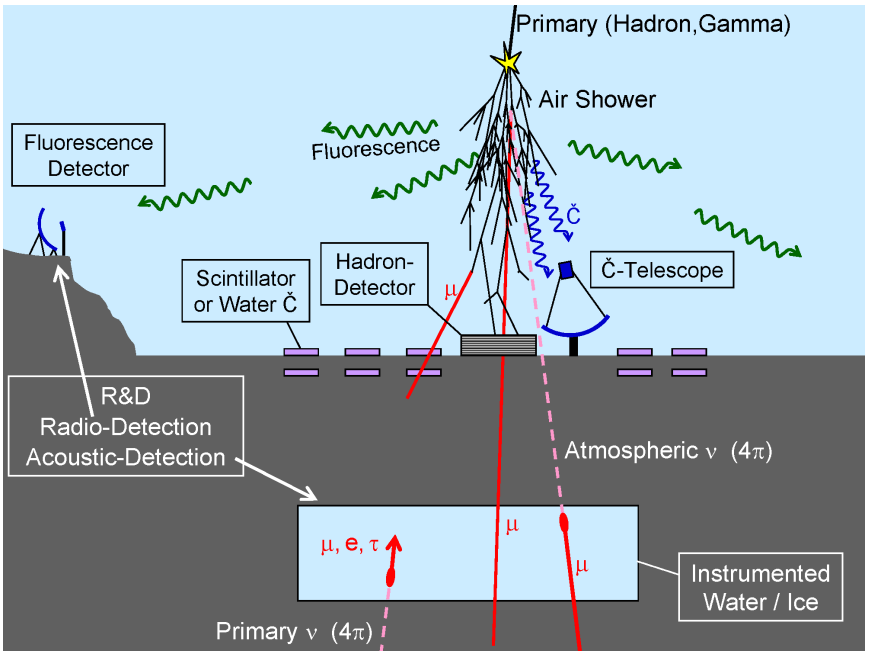

Figure 16: Sketch of experimental techniques for ground-based detection of high-energy charged cosmic rays, gamma rays and neutrinos.

power between gamma ray showers and hadronic showers make them the currently most powerful instruments for ground based gamma ray astronomy.
Finally, cosmic neutrinos are detected by their interaction in instrumented deep-underground water or ice volumes. Muons, produced by interaction of muon neutrinos, and showers ("cascades"), produced by electron and tau neutrinos, are detected by measuring the emitted Cherenkov light. In addition, radio and acoustic detection techniques for neutrino interactions are under development. Background of atmospheric muons, created in air showers, can be eliminated by restricting the field of view for muon neutrinos to the lower hemisphere, such as to use the earth as shielding.
Figure 17 shows the layout of the Pierre Auger Observatory, todays largest detector for cosmic rays, presently under construction in the Pampa Amarilla in Argentina. AUGER is a hybrid detector, combining a 3000 km^2 surface array of 1600 water Cherenkov tanks with 4 fluorescence sites, each equipped with 6 telescopes. It is specialized to explore the cosmic rays at the end of the energy scale and answer the question whether the spectrum continues beyond 10^{20} eV or whether it breaks due to a cut-off mechanism. This example underlines the dramatic differences between the size of detectors and the microscopic volumes in which the hard interactions of highest energy particles take place.

6 Conclusions

Particle detectors are high technology devices which localize particles in position, momentum, energy, time, charge and mass on the basis of particle interactions

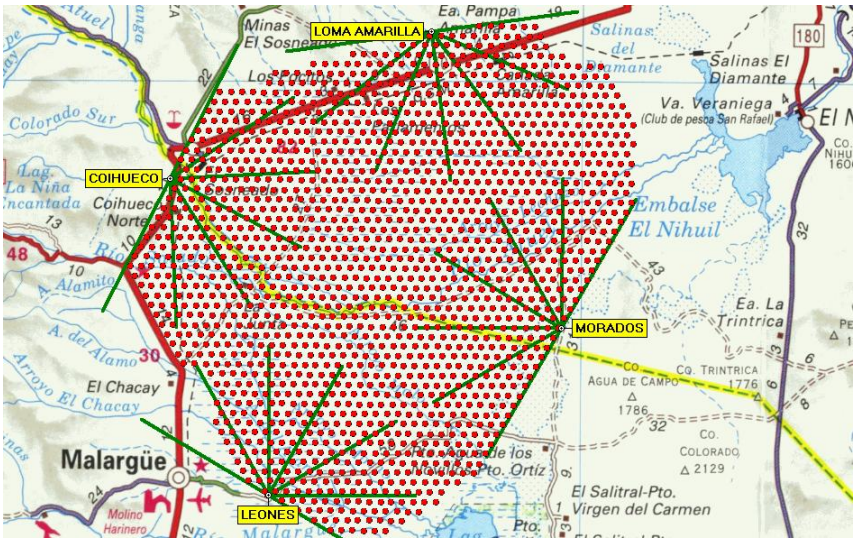

Figure 17: Layout of the Pierre Auger Observatory in the Pampa Amarilla in Argentina (http://www.auger.org). The dots are water Cherenkov tanks. The locations of the four fluorescence sites are shown and the angles covered by the individual telescopes are indicated by lines.

in the detector material. They operate in the deeply classical regime so that particles can be interpreted as classical objects following classical trajectories. Tails of wave functions are neither affected in the preparation step in particle accelerators nor in the measurement process in detectors. However, the final state particles observed in detectors are often not those which are being studied or which are involved in hard interactions on short length scales. Nevertheless, quantum field theory can be precisely tested on sub-femtometer length scales by measuring final state particles at length scales of meters or even kilometers, if a large data set of final states is analyzed statistically. The analogy is the double slit experiment for electron diffraction, where a diffraction pattern becomes visible only after measuring many electrons passing the slits, finally allowing to test the scattering dynamics and the structure of the target (the double slit).
Even though the notion of relativistic particles is problematic in quantum field theory, particle detectors are visualizing an asymptotic situation in which the classical particle concept is applicable and particles become visible in a completely intuitive fashion.

References

Cronin, J./Gaisser, T. K./Swordy, S. P.: The Most Energetic Particles in the Universe. Scientific American **276** (1997), p. 44 20

Eidelman, S. et al.: Review of Particle Physics. Physics Letters B **592** (2004), p. 1 3

Fredenhagen, K./Rehren, K.-H./Seiler, E.: Quantum Field Theory: Where We Are. 2006, hep-th/0603155 2

Hegerfeld, G. C.: In Lukierski, J./Rembieliński, J., editors: New Developments in Fundamental Interaction Theories, AIP Conference Proceedings 589. Melville, NY: AIP, 2001, pp. 357 – 366 2